Agnieszka NIEDŹWIEDZKA, Seweryn LIPIŃSKI
FACULTY OF TECHNICAL SCIENCES, UNIVERSITY OF WARMIA AND MAZURY IN OLSZTYN
11 Oczapowskiego St., 10-736 Olsztyn, Poland

Validation of Numerical Simulations of Cavitating Flow in Convergent-Divergent Nozzle

Abstract

In the article, validation of results of numerical simulations of cavitating flow in a convergent-divergent nozzle is presented. In validation, a new optoelectronic system is used in order to extract the changes in the bubbles volume fraction of the mixture in freely specified cross-sections. Three homogeneous models (Schnerr and Sauer, Singhal et al. and Zwart et al.) are analysed. The assessment of usefulness of the new system in experimental measurements of cavitation is the main aim of the article. Looking for new opportunities to replace image analysis, which is a traditional validation method in numerical simulations of cavitating flows, is motivation for the research. The results obtained with the use of the system show a good agreement with the simulation's results for the two chosen cross-sections. The described optoelectronic system gives promising results and can be regarded as an alternative to traditional validation methods in the cavitation research area.

Keywords: cavitating flow, numerical simulations, homogenous models, optoelectronic validation.

1. Introduction

The cavitation phenomenon is one of the most exploited topics in the area of research on fluid flow. It consists in growth of vapour bubbles of a given fluid under the influence of drop in pressure below the saturated liquid pressure. Cavitation is common not only in fluid machinery, but also in hydraulics systems. The main reason for interest from scientists is cavitation erosion, which accompanies this phenomenon. It causes inter alia surface damage, noise and vibrations [1-3]. The best solution would be completely avoiding of cavitation what is unfortunately impossible. However, within our capabilities is numerical prediction of this phenomenon. The better the assessment level between prediction and experimental results, the better is perspective to find measures decreasing its negative influence. Knowledge of the location of the areas, where cavitation has high intensity, could be a hint for designers to improve the material properties in these places or to make changes in the construction to minimalize the risk of destruction.

To obtain information about the assessment level, two basic tools are necessary. One of them is software with an algorithm concerning the mathematical description of cavitation; the other is system collecting data for validation process. The oldest and most prevalent method in experimental investigation is high-speed photography. It allows registering the changes in dimensions and intensity of cavitation area within a specified time. The obtained images should be qualitatively and quantitatively analysed [4-6]. Over time, the holography was introduced also for that purpose [7, 8]. In cavitating flow measurements, Particle Image Velocimetry (PIV) application can also be found, which is common particularly in flow analyses. This system allows a really precise monitoring of the trajectory of fluid molecules [9, 10]. To other methods belong method applying double optical probe and X-ray [11-14]. Double optical probe is used to extract the local void fraction of liquid-vapour mixture. Using this tool is connected with the interference in the considered system, which can cause disturbances in the analysed flow [11-13]. X-ray measurements do not give answer about the forming of cavitating flow in a specified period and are controversial because of the potential risk connected with the harmful radiation [14]. The choice of the method, which is most suitable for the specified problem, depends on the laboratory stand construction and on the financial abilities. To the other considered aspect belong measurement accuracy, safety and usefulness of the obtained data, especially in relation to the numerical simulations results.

2. Theoretical background

There are many methods applied in numerical simulations of cavitating flows. The most common method is the so-called one-fluid method with the homogeneous approach. In this method, fluid is a mixture of liquid and its vapour with an averaged density. The governing equations for mass, momentum and energy are:

$$\frac{\partial \rho}{\partial t} + div(\rho \vec{u}) = 0 \tag{1}$$

$$\frac{\partial \rho}{\partial t}(\rho \vec{u}) + div(\rho \vec{u} \otimes \vec{u}) = div\left(-p\overleftrightarrow{I} + \overleftrightarrow{\tau}^m + \overleftrightarrow{\tau}^R\right) + \rho \vec{s}_b \tag{2}$$

$$\frac{\partial \rho}{\partial t}(\rho e) + div(\rho e \vec{u} + \rho \vec{u}) = div[(\overleftrightarrow{\tau}^m + \overleftrightarrow{\tau}^R)\vec{u} + \vec{q}^m + \vec{q}^R] + \rho \vec{s}_e, \tag{3}$$

where: ρ – liquid density, kg/m^3, t – time, s, u – velocity. m/s, p – local fluid pressure. Pa, $\overleftrightarrow{\tau}^m$ – viscous molecular stress tensor, kg/(m·s^2), $\overleftrightarrow{\tau}^R$ – turbulent Reynolds stress tensor, kg/(m·s^2), $\vec{s}_b$ – intensity of the mass forces source, N/m^3, e – energy, J, $\vec{q}^m$ – molecular heat flux, kg/(m·s^2), $\vec{q}^R$– turbulent heat flux, kg/(m·s^2), $\vec{s}_e$ – intensity of the energy source, N/m^3, are solved for all phases together [15, 16].

For the homogeneous approach, the additional transport equation is characteristic. In the most cases this transport equation bases on the bubble dynamic equation presented by Plesset [17]:

$$R\frac{d^2R}{dt^2} + \frac{3}{2}\left(\frac{dR}{dt}\right)^2 = \frac{p_{sat}-p}{\rho_l} - \frac{2\sigma}{\rho_l R} - 4\frac{\mu_l}{\rho_l R}\frac{dR}{dt}, \tag{4}$$

where: R – the initial bubble radius, m, p_{sat} – saturation vapour pressure, Pa, ρ_l – liquid density, kg/m^3, σ – surface tension, N/m, μ_l – liquid dynamic viscosity, Pa·s. Generally, the transport equation is expressed in terms of change of vapour volume:

$$\frac{\partial \alpha_v}{\partial t} + div(\alpha_v \vec{u}) = \Delta\alpha, \tag{5}$$

where: α – void fraction, dimensionless, α_v – vapour void fraction, dimensionless. The transport equation is expressed in form of mass transfer rates (called source terms):

$$\dot{m} = \begin{cases} \dot{m}^+ & if\ p > p_{sat} \\ \dot{m}^- & if\ p < p_{sat} \end{cases}, \tag{6}$$

that have different forms for condensation (increase of liquid mass $\dot{m}^+$), when the local fluid pressure increases above the saturated vapour pressure and evaporation (decrease of liquid mass $\dot{m}^-$), when the local fluid pressure drops below the saturated vapour pressure.

The history of homogeneous models started in 1992. In this year, Kubota et al. presented first model called Local Homogeneous Model (LHM) [18]. Because of its instability scientists started to look for another version of source terms. Until today more than twenty models has been published [19-25]. Several works present a summary of the most important source term [3, 26-30]. The most detailed description of the homogeneous models contains the work by Niedźwiedzka et al. [30].

In the presented article, three homogeneous models are analysed: Schnerr and Sauer, Zwart et al., and Singhal et al. Schnerr and Sauer presented their model of transport equation in 2001 [23]. This model do not have condensation and evaporation constants. It requires only quantitative values of the physical parameters. The source terms of the transport equations for condensation ($\dot{m}^+$) and evaporation ($\dot{m}^-$) are formulated as follows:

$$\dot{m}^+ = \frac{\rho_v \rho_l}{\rho_m} \alpha_v (1-\alpha_v) \frac{3}{R} \sqrt{\frac{2}{3}\frac{(p-p_{sat})}{\rho_l}} \tag{7}$$

$$\dot{m}^- = -\frac{\rho_v \rho_l}{\rho_m} \alpha_v (1-\alpha_v) \frac{3}{R} \sqrt{\frac{2}{3}\frac{(p-p_{sat})}{\rho_l}}, \tag{8}$$

where: ρ_v – vapour density, kg/m^3, ρ_m – mixture density, kg/m^3.

The next used model is Singhal [24]. This model, called Full Cavitation Model, was formulated in 2002 and became the first commercially used. Its form of source terms takes into account the content of more constituents than other, shown above, solutions. The mass transfer rates for condensation ($\dot{m}^+$) and evaporation ($\dot{m}^-$) have a following form:

$$\dot{m}^+ = C_p \frac{\sqrt{k}}{\sigma} \rho_l \rho_l \sqrt{\frac{2}{3}\frac{(p-p_{sat})}{\rho_l}} \tag{9}$$

$$\dot{m}^- = -C_d \frac{\sqrt{k}}{\sigma} \rho_l \rho_v \sqrt{\frac{2}{3}\frac{(p-p_{sat})}{\rho_l}} \left(1 - f_v - f_g\right), \tag{10}$$

where: C_p – condensation constant, dimensionless, C_d – evaporation constant, dimensionless, k – local turbulent kinetic energy, m^2/s^2, f_v – vapour mass fraction, dimensionless, f_g – noncondensible gases mass fraction, dimensionless.

Zwart et al. [25] presented their homogeneous model in 2004. In this model, the vapour volume fraction in the evaporation rate is replaced with the product of the nucleation site of volume fraction (α_{nuc}) and the remaining fluid volume fraction ($1-\alpha_v$). The source terms of model proposed by Zwart et al. are expressed in a following form:

$$\dot{m}^+ = C_p \frac{3\alpha_v \rho_v}{R} \sqrt{\frac{2}{3}\frac{(p-p_{sat})}{\rho_l}} \tag{11}$$

$$\dot{m}^- = -C_d \frac{3(1-\alpha_v)\alpha_{nuc}}{R} \sqrt{\frac{2}{3}\frac{(p-p_{sat})}{\rho_l}}. \tag{12}$$

3. Experimental Setup

The test rig is shown in Fig. 1. Its detailed description can be found in [31].

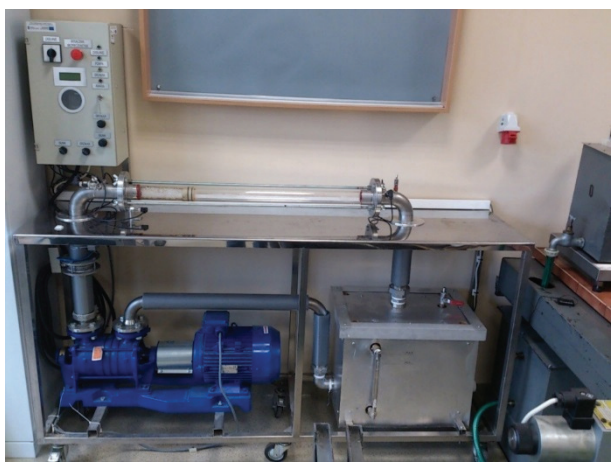

Fig. 1. The test rig [31]

The test rig is coupled with an optoelectronic registration system (Fig. 2). Its construction bases on lasers and photoresistors. These are placed in specified cross-sections in order to extract changes in the bubbles volume fraction of the mixture. The idea of the measurements bases on the assumption that cavitation leads to diffusion of lasers light on the vapour bubbles.

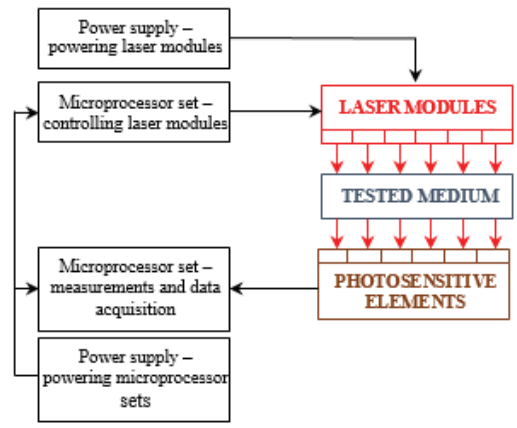

Fig. 2. The diagram of the registration system

The analysed geometry of the converging-diverging nozzle is presented in Fig. 3. The angles of converging and diverging sections have both 45°. The throat has diameter of 3 and length of 6 mm. The outside diameter of the nozzle is 50 mm.

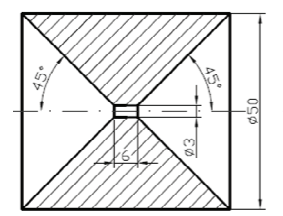

Fig. 3. Cross-section of the analysed converging-diverging nozzle [31]

4. Numerical Simulations

Unsteady two-dimensional numerical simulations were carried out in Fluent software (Ansys 14.5). Models presented in the section 2 are available from Fluent interface. Vapour volume fraction's prediction in the specified cross-section is the aim of the numerical calculations. The specified value of time step is 0.001 s. The average inlet velocity is 0.5 m/s.

The geometry of the area analysed in the simulation process is presented in Fig. 4. The total length of the area is 523 mm. The distance from the left edge of the system to the left edge of the nozzle is 70 mm. The analysed cross-sections are placed 60, 120 and 180 mm behind the right edge of the nozzle.

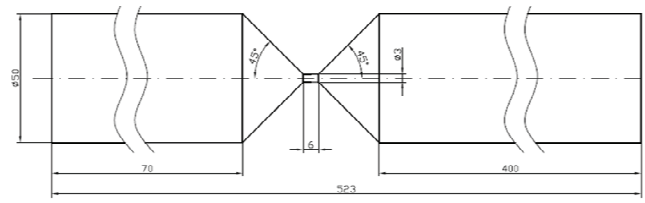

Fig. 4. The geometry of the analysed area

Using ICEM CFD, the structural quadrangle mesh was implemented. In the numerical simulations, three mesh levels are considered. The refinement scale is power of two and four of the

basic cell structure. The detailed information about the mesh is presented in Tab. 1.

Tab. 1. Mesh properties

	Mesh level 1	Mesh level 2	Mesh level 3
Total elements	1244	4170	16898
Total nodes	1092	4175	16317
Min. surface area, mm^2	0.086	0.019	0.004
Max. surface area mm^2	78.092	19.523	4.880
Mean surface area mm^2	24.863	6.216	1.554

5. Results and discussion

The timeframe for numerical simulations is 1 s. Fig. 5a-5c present the results of vapour volume fraction's changes for the three chosen models and three specified mesh levels. From the analysis of the results obtained using Schnerr and Sauer model can be concluded that the changes have a regular character - it is the best visible for the second mesh level. Along with increasing mesh density grows the maximum value of vapour volume fraction - from 0.012 to 0.018 (Tab. 2).

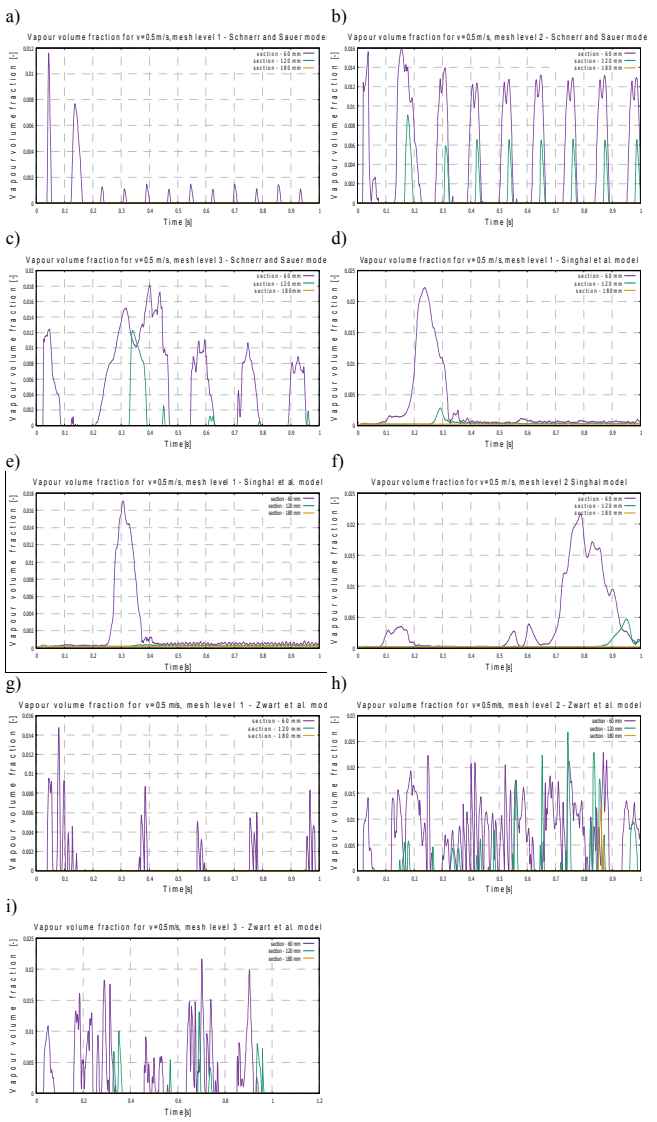

Fig. 5. Changes in vapour volume fraction in time of 1 s for Schnerr and Sauer model (5a – 1st mesh level, 5b – 2nd mesh level, 5c – 3rd mesh level), Singhal et al. model (5d – 1st mesh level, 5e – 2nd mesh level, 5f – 3rd mesh level) and Zwart et al. model (5g – 1st mesh level, 5h – 2nd mesh level, 5i – 3rd mesh level)

In analyses made using Singhal et al. model (Fig. 5d-5f), the periodic character of phenomenon is no more visible. Increase of mesh density do not have big influence on the maximum value of vapour volume fraction, which is about 0.2 (Tab.2). From the analysis of the diagrams obtained using Zwart et al. model (Fig. 5g-5i) can be concluded that the changes do not have a regular character, but unlikely the results shown in Fig. 5d-5f, more than one peak is marked. The maximum value of vapour volume fraction varies from 0.015 to 0.027 (Tab. 2). For all the diagrams common is that maximum values of vapour volume fraction for the first cross-section are noticeable and minimum values are noted for the third cross-sections.

Tab. 2. Maximum values of vapour volume fraction for the chosen models and specified mesh level.

	Mesh level 1	Mesh level 2	Mesh level 3
Schnerr and Sauer	0.012	0.016	0.018
Singhal et al.	0.023	0.017	0.022
Zwart et al.	0.015	0.027	0.022

The optoelectronic system do not give a direct answer about the content of vapour in the analysed fluid. The obtained information is the change of the voltage measured on the photoresistors. The simplest validation method is comparison of the shapes of the passages achieved from numerical simulations and experimental data. Fig. 6a – 6c present the juxtaposition of the data from numerical calculations with the voltage signal measured on the photoresistors for the first, second and third cross-sections, respectively. Interpretation of the diagrams obtained from numerical simulations is simple. Higher above the basic level the peaks, vapour fraction is forming. The analysis of voltage signal requires another approach. The voltage signal decreases because of light diffusion on the vapour bubbles and a larger vapour fraction in the analysed cross-section results in more significant signal decrease.

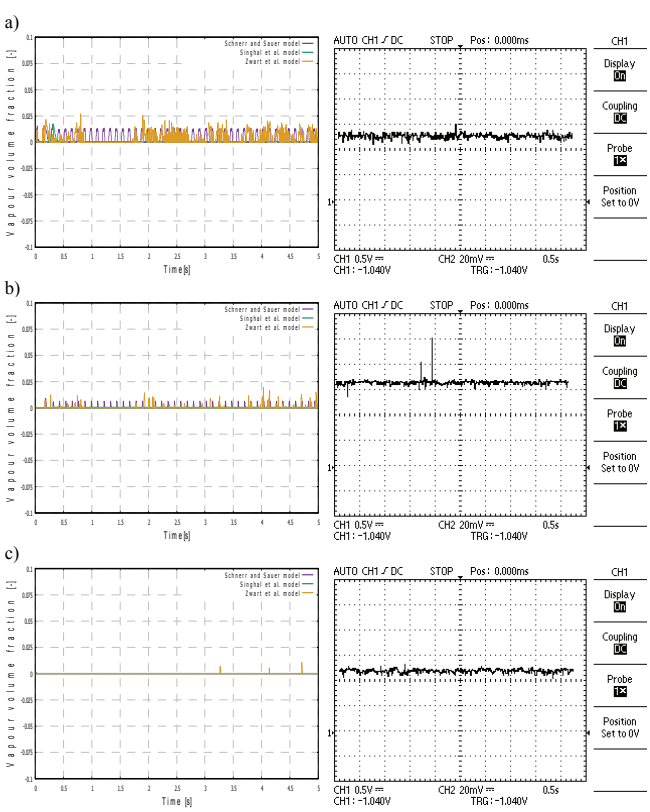

Fig. 6. Comparison of vapour volume fraction and the voltage signal for the cross-section: a) the first, b), the second, c) the third

From the comparison of vapour volume fraction from numerical simulations with the voltage signal for the appropriate cross-sections it can be concluded that in case of the first and second cross-sections a close relationship between the graphs is observable.

6. Conclusions

Based on the analysis of the results of numerical simulations and experimental measurements the following concluding remarks can be drawn:

- a new approach in cavitation diagnostics is presented;
- the shape of cavitation cloud to the second status is relegated, the main role plays vapour volume fraction;
- comparison of the vapour volume fraction from numerical simulations and the voltage signal from measurements shows a good coherence for the first and the second (out of three) analysed cross-sections;
- three-dimensional analyses should be considered in further steps;
- the new validation method seems to be useful and should be further investigated.

7. References

[1] Ashrafizadeh S. M. and Ghassemi H.: Experimental and numerical investigation on the performance of small-sized cavitating venturis. Flow Measurements and Instrumentation, vol. 42, pp. 6-15, 2015.

[2] Crum. L.A.: Nucleation and stabilization of microbubbles in liquids. Applied Scientific Research, vol. 38, pp. 101-115, 1982.

[3] Frikha S., Coutier-Delgosha O. and Astolfi J. A.: Influence of the cavitation model on the simulation of cloud cavitation on 2D foil section. International Journal of Rotating Machinery, 146234, 2008.

[4] Ausoni P., Zobeiri A., Avellan F. and Farhat M.: The effects of a tripped turbulent boundary layer on vortex shedding from a blunt trailing edge hydrofoil. Journal of Fluids Engineering, vol. 134(5), 051207, 2012.

[5] Kravtsova A. Y., Markovich D. M., Pervunin K. S., Timoshevskiy M. V. and Hanjalić K.: High-speed imaging of cavitation regimes on a round-leading-edge flat plate and NACA0015 hydrofoil. Journal of visualization, vol. 16(3), pp. 181-184, 2013.

[6] Timoshevskiy M. V., Churkin S. A., Kravtsova A. Y., Pervunin K. S., Markovich D. M. and Hanjalić K.: Cavitating flow around a scaled-down model of guide vanes of a high-pressure turbine. International Journal of Multiphase Flow, vol. 78, pp. 75-87, 2016.

[7] Katz J. and Acosta A.. Observations of nuclei in cavitating flows. Applied Scientific Research, vol. 38, pp. 123-132, 1982.

[8] Lauterborn W.: Cavitation bubble dynamics—new tools for an intricate problem. Applied Sci. Research, vol. 38, pp. 165-178, 1982.

[9] Dular M., Bachert R., Stoffel B. and Širok B.: Experimental evaluation of numerical simulation of cavitating flow around hydrofoil. European Journal of Mechanics-B/Fluids, vol. 24, pp. 522-538, 2005.

[10] Kravtsova A. Y., Markovich D. M., Pervunin K. S., Timoshevskiy M. V. and Hanjalić K.: High-speed visualization and PIV measurements of cavitating flows around a semi-circular leading-edge flat plate and NACA0015 hydrofoil. International Journal of Multiphase Flow, vol. 60, pp. 119-134, 2014

[11] Barre S., Rolland J., Boitel G., Goncalves E. and Patella R. F.: Experiments and modeling of cavitating flows in venturi: attached sheet cavitation. European Journal of Mechanics-B/Fluids, vol. 28, pp. 444-464, 2009.

[12] Coutier-Delgosha O., Devillers J. F., Pichon T., Vabre A., Woo R. and Legoupil S.: Internal structure and dynamics of sheet cavitation. Physics of Fluids, vol. 18, 017103, 2006.

[13] Stutz B. and Reboud J. L.: Measurements within unsteady cavitation. Experiments in Fluids, vol. 29(6), pp. 545-552, 2000.

[14] Stutz, B. and Legoupil, S.: X-ray measurements within unsteady cavitation. Experiments in Fluids, vol. 35(2), pp. 130-138, 2003.

[15] Liu T. G., Khoo B. C. and Xie W. F.: Isentropic one-fluid modelling of unsteady cavitating flow. Journal of Computational Physics, vol. 201 (1), pp. 80-108, 2004.

[16] Sobieski W.: The basic equations of fluid mechanics in form characteristic of the finite volume method. Technical Sciences, vol. 14, pp. 299-313, 2011.

[17] Plesset M. S. and Prosperetti A.: Bubble dynamics and cavitation. Annual Review of Fluids Mechanics, vol. 9, pp. 145-185, 1977.

[18] Kubota A., Kato H. and Yamaguchi H.. A new modeling of cavitating flows: a numerical study of unsteady cavitation on a hydrofoil section. Journal of Fluid Mechanics, vol. 240, pp. 59-96, 1992.

[19] Huang B. and Wang G. Y.: A modified density based cavitation model for time dependent turbulent cavitating flow computations. Chinese Science Bulletin, vol. 56, pp. 1985-1992, 2011.

[20] Iben U.: Modeling of cavitation. Systems Analysis Modeling Simulations, vol. 42, pp. 1283-1307, 2002.

[21] Kunz R. F., Bogger D. A., Chyczewski T. S., Stinebring D. R. and Gibeling H.J.: Multi-phase CFD analysis of natural and ventilated cavitation about submerged bodies. Third ASME/JSME Joint Fluids Engineering Conference (FEDSM'99), vol. 99(1), 1999.

[22] Merkle C. L., Feng J. and Buelow P. E. O.: Computational modeling of the dynamics of sheet cavitations. Third International Symposium on Cavitation (CAV'03), 1998.

[23] Schnerr G. H. and Sauer J.: Physical and numerical modeling of unsteady cavitation dynamics. Fourth International Conference on Multiphase Flow (ICMF'01), 2001.

[24] Singhal A. K., Athavale M. M., Li H. and Jiang Y.. Mathematical basis and validation of the full cavitation Model. Journal of Fluids Engineering, vol. 124, pp. 617-624, 2002.

[25] Zwart P. J., Gerber G. and Belamri T.: A two-phase flow model for prediction cavitation dynamics. ICMF 2004 - International Conference on Multiphase Flow, 2004.

[26] Goel T., Thakur S., Haftka R., Shyy W. and Zhao J.: Surrogate model-based strategy for cryogenic cavitation model validation and sensitivity evaluation. International Journal for Numerical Methods in Fluids, vol. 58, pp. 969-1007, 2008.

[27] Goncalves E. and Charrière B.: Modeling for isothermal cavitation with a four-equation model. International Journal of Multiphase Flow, vol. 59, pp. 54-72, 2014.

[28] Senocack I. and Shyy W.: Numerical simulation of turbulent flows with sheet cavitation. Proceedings of the Fourth International Symposium on Cavitation (CAV2001), Pasadena, USA, 2001.

[29] Žnidarčič A., Mettin R. and Dular M.: Modelling cavitation in a rapidly changing pressure field – application to a small ultrasonic horn. Ultrasonic Sonochemistry, vol. 22, pp. 482-492, 2015.

[30] Niedźwiedzka A., Schnerr G. H. and Sobieski W.: Review of numerical models of cavitating flows with the use of the homogeneous approach. Archives of Thermodynamics, 2016, in press.

[31] Niedźwiedzka A. and Sobieski W.: Experimental investigations of cavitating flows in a Venturi tube. Technical Sci., vol. 19(2), 2016.

Received: 10.07.2016 *Paper reviewed* *Accepted: 01.09.2016*

Agnieszka NIEDZWIEDZKA, MSc

Graduate of the Faculty of Technical Sciences of the University of Warmia and Mazury in Olsztyn. Student of the third year PhD studies in area of agricultural engineering at the University of Warmia and Mazury in Olsztyn. Research interests include numerical simulations of mechanical processes, especially cavitation phenomenon.

e-mail: agnieszka.niedzwiedzka@uwm.edu.pl

Seweryn LIPIŃSKI, PhD

Graduate of the Faculty of Electronics, Telecommunications and Informatics of the Gdansk University of Technology. Works in the Department of Electrical and Power Engineering, Electronics and Automation of the University of Warmia and Mazury in Olsztyn. Research interests include inter alia the use of methods of signal and image processing and applications of electronics in many areas, including medicine, mechanics and agricultural engineering.

e-mail: seweryn.lipinski@uwm.edu.pl